ELECTROMAGNETICALLY ENHANCED FILTRATION OF ALUMINUM MELTS

Mark William Kennedy[1], Shahid Akhtar[1], Jon Arne Bakken[1], Ragnhild E. Aune[1,2]

[1]Department of Materials Science and Engineering, Norwegian University of Science and Technology, N-7491 Trondheim NORWAY
[2]Department of Materials Science and Engineering, Royal Institute of Technology, 100 44 Stockholm, SWEDEN
Communicating author: ragnhild.aune@ntnu.no

Keywords: Aluminum, Ceramic Foam Filters, Magnetic Field, Meniscus, Coil

Abstract

The major drawback of the use of Ceramic Foam Filters (CFF) for purification of aluminum is their low efficiency for particles in the range of 10-30 µm. The application of electromagnetic force from an induction coil in combination with a filter can cause back mixing and recirculation through the filter media. In the present work an experimental set-up has been designed, built and verified by studying the meniscus behavior of molten aluminum under varying magnetic field strength. Batch type filtration experiments with 30 ppi CFF were also conducted with and without a magnetic field using an A356 aluminum alloy containing 20% anodized and lacquered plates, as well as 20% composite material (A356 base and 15% SiC particles with size range 10-50 µm). The presence of a magnetic field has proven to have both an effect on the build up of the filter cake, as well as on the re-distribution of particles within the filter.

Introduction

Due to increased demand for clean high-performance aluminum products, it has become an increasingly important task to reduce the level of impurities, and especially inclusions, in aluminum melts. It is a well known fact that non-metallic inclusions not only form porosity, but also result in stress concentration, which in turn may affect the static and dynamic properties of aluminum alloy products[1-2]. Traditional processes such as gravity sedimentation/flotation, degassing, flux refining and filtration, have difficulty meeting the cleanliness levels demanded in many applications, due to their low efficiency in removing micrometer-sized inclusions[3].

El-Kaddah *et.al*[4] presented the concept of combining electromagnetic separation with filtration to enhance the inclusion removal efficiency. They did, however, not provide sufficient experimental verification of the idea.

In the present work an experimental set-up including several different induction coils has been designed and verified with respect to the generation of magnetic pressure and hence flow using a 50 Hz AC field. The molten metal meniscus behavior has also been studied as a way of directly evaluating the influence of the magnetic field on the molten metal sample. Different coil designs and a number of different currents were used. It was hoped to qualitatively observe mixing, the size of the meniscus and how great a magnetic pressure that could be developed, without damaging the apparatus or excessive overheating the molten aluminum. In order to demonstrate the effect of back mixing of the fluid through the filter media, batch filtration tests have been conducted with and without a magnetic field.

Theory

The use of electromagnetic fields is an emerging technology for the production of high-quality aluminum alloys with increased melt cleanliness[5]. Electromagnetic fields provide a means of influencing separation processes, without physical contact and added risk of contamination. The liquid metal will be acted upon by the electromagnetic Lorentz force $\vec{F}$ (N/m^3) inducing motion:

$$\vec{F} = \vec{J} \times \vec{B} \qquad (1)$$

where $\vec{J}$ is the induced current density (A/m^2), and $\vec{B}$ the magnetic flux density (also simply referred to as the magnetic field (T)). In addition to generating motion the electromagnetic field will also heat the metal.

The convective flow induced in the liquid metal by the axial variation of the electromagnetic field of a short coil, may adversely affect the separation process[6]. In Figure 1, the variation of the axial magnetic field along the coil length for various coil diameters to length ratios, evaluated using the Biot-Savart Law for an empty coil, are presented. It can be seen in Figure 1, that longer coils give a more powerful magnetic field, which can be very homogenous over much of their length, but with significant end effects. Shorter coils give less axial variation and overall weaker fields, as well as more radial variation of the magnetic field strength (not shown). The possible impact this has on the separation process is not clear; however, it could be expect that a very short coil behaves differently from a very long coil.

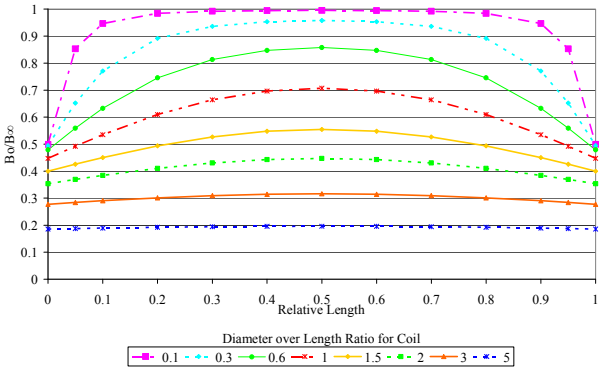

Figure 1. Relative (short coil/equivalent length of infinite coil) axial magnetic flux density for an empty coil is plotted against the shape at constant current and turns per unit length.

In a short coil, the presence of the work piece alters the strength of the axial component of the magnetic field in the air gap, due to the reduced coil aperture. Kennedy *et. al.*[7] have successfully used Equation (2) to estimate the strength of the axial magnetic flux density in a short coil, accounting for the length of the coil and the presence of the work piece:

$$B_0^* = k_N^* B_\infty = k_N^* \mu_o H_\infty = k_N^* \mu_o N_c I_c / \ell_c \qquad (2)$$

where B_0^* is the axial magnetic flux density in the air gap of a short coil containing a work piece (T), B_∞ the magnetic flux density of an equivalent length of infinite coil without a work peice (T), k_N^* a modified shortness correction factor for a loaded coil, μ_o is the magnetic permiability of free space = 4 π 10^{-7} H/m, N_c is the number of coil turns, I_c is the coil current (A) and ℓ_c is the length of the coil (m).

Vaughan and Williamson[8] developed an equation for a modified short coil correction factor, to account for the presence of the work piece:

$$k_N^* = k_N (1 - [D_w / D_c]^2) + [D_w / D_c]^2 \qquad (3)$$

where k_N is the Nagaoka coefficient, D_w the diameter of the work piece (m), and D_c the diameter of the coil (m). The Nagaoka coefficient is a theoretical factor, which accounts for the reduced strength of the magnetic field in an empty short coil and it has been tabulated elsewhere [9-10].

For the dimensions of typical induction coils, the Nagaoka coefficient can be conveniently estimated by the Wheeler formula[11] as reformulated by Knight[12]:

$$k_N = 1/[1 + 0.4502 (D_c + \delta_c) / \ell_c)] \qquad (4)$$

where δ_c is the electromagnetic penetration depth in the coil (m).

The magnetic flux density in the air gap is extremely important as it directly relates to the magnitude of the electromagnetic pressure P_m (Pascals) that can be developed as follows:

$$P_m = B_0^{*2} / (2 \mu_o \mu_r) \qquad (5)$$

One problem associated with the electromagnetic separation techniques is the difficulty in generating large Lorentz forces deep within a highly conductive metal. This is especially true for AC fields at high frequencies, due to the skin effect:

$$\delta = (\rho/[\pi f \mu_o \mu_r])^{0.5} \qquad (6)$$

where ρ is the electrical resistivity (ohm m), f the frequency (Hz) and μ_r is the relative permeability of the metal (1 for aluminum).

The electromagnetic penetration depth (δ) is reduced in proportion to the square root of the frequency ($1/\sqrt{f}$), as presented in Figure 2 and Equation (6). As can be seen from Figure 2, the penetration depth becomes very small at high frequency, e.g. ~1 mm for pure liquid aluminum at 100 kHz, while at mains frequencies of 50 or 60 Hz, it is ~35 mm. For magnetically thick samples (*Radius/δ>3*) the magnetic flux density declines nearly exponentially with each penetration depth, resulting in that only a negligible flux remains after about 3 penetration depths. As a result of this, it is therefore not possible to produce significant Lorentz forces deep within a thick work piece of a high conductivity metal at high frequency.

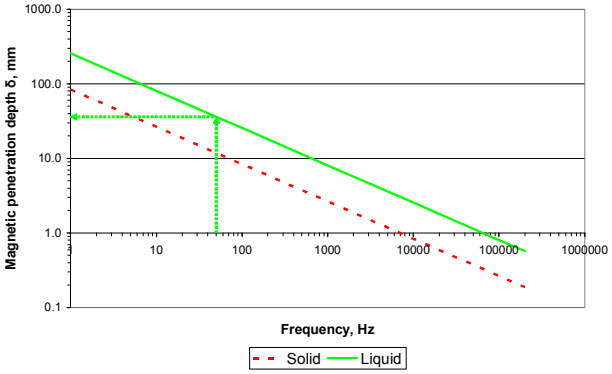

Figure 2. The electromagnetic penetration depth is plotted against the frequency for solid and liquid aluminum.

The use of high frequency does, however, improve the efficiency of induction heating by increasing the ratio of (*Radius/δ*) for a fixed work piece radius. Overheating of the work piece will then limit the amount of current and hence the magnitude of the magnetic field that can be effectively used.

Conducting experiments at mains frequencies, i.e. 50 or 60 Hz, have therefore the following significant advantages:

- deep electromagnetic penetration, and
- powerful magnetic fields without overheating of the work piece.

Experimental

Set Up

Two separate coil designs were produced for use with the meniscus and batch experiments. One coil was a traditional "long" coil (Coil 1), and the other an unusual multi-layer "short" coil (Coil 2), as pictured in Figures 3 a) and b). The multi-layer coil was specifically designed to produce the most powerful magnetic field possible over the desired length of the sample, using the available power supply. The specifications for the coils are given in Table I.

Table I. Specifications for the long (Coil 1) and multi-layer coil (Coil 2).

Coils:	Coil 1 Expt 2	Coil 2 2-1	Coil 2 2-2	Coil 2 2-3	Coil 2 2-1 + 2-2	Coil 2 2-2 + 2-3
Inside diameter, mm	118	126	140	153	126	140
Average diameter, mm	124	132	146	159	132	146
Height, mm	300	104	105	105	107	108
Coil copper tube diameter, mm	6.35	6	6	6	6	6
Coil copper tube thickness, mm	0.762	1	1	1	1	1
Number of turns	41.0	15.5	15.5	15.5	31.0	31.0
Measured inductance of empty coil, μH	71.7	25.1	29.0	33.2	103.3	119.9
Measured resistance at maximum load, ohms	0.0319	0.00928	0.01018	0.01126	0.01962	0.02193
Avg. Coil temperature at maximum load, Deg C:	62	23	23	25	23	27

The various sub-coils in Coil 2 could be placed in series or parallel to achieve the most advantageous configuration. The strongest magnetic fields (~0.2 T), as well as the most stable thermal operation, were achieved when the two inner coils were electrically connected in series and operated at the maximum available voltage (~28 V) with the water cooling in parallel and flowing counter currently. A cooling water flow of approximately 3-4 m/s was obtained at 4-6 Bar line pressure.

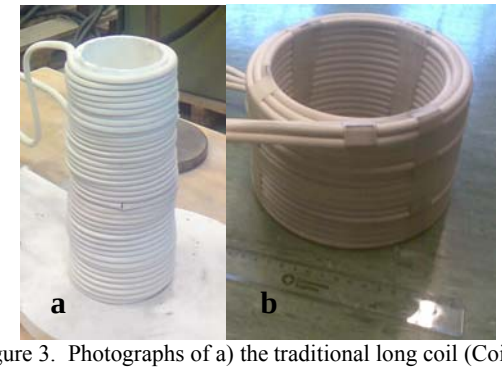

Figure 3. Photographs of a) the traditional long coil (Coil 1), and b) the multi-layer coil (Coil 2).

The transformer used as the power supply was limited to a nominal voltage of 30 V and a maximum of 1500 A. Due to the high resistance of the coils, it was not necessary to compensate the power factor on the secondary side using a capacitor bank. Electrical measurements were conducted using a Fluke 43B Power Quality Analyzer. In Experiments 1 and 2, a 500 A Fluke current probe was used. This probe was however, replaced with a Fluke i1000s AC current probe, with an accuracy of 1% and a precision of 1 A, on all subsequent experiments. The amount of energy entering the liquid metal was determined by subtracting the power lost in the coil (measured empty) from the total power of the system while operating with liquid metal. Electrical values were qualitatively verified using batch calorimetric measurements, which agreed within the accuracy of ~ 5%. For Experiment 2, the obtained values for the current, as well as the power are only indicative as the current probe was used outside of its linear range (readings were later adjusted by calibration against the i1000s probe).

The experimental apparatus were constructed using two lengths of BIMEX 400 fiber riser supplied by Intermet Refractory Products Ltd., with a nominal inside diameter of 102 mm, an outside diameter of 120 mm, and a length of 150 mm. The two lengths were joined together using Fibrefrax moldable cement. The bottom portion of the apparatus was imbedded in a sand mold to provide a leak free bottom.

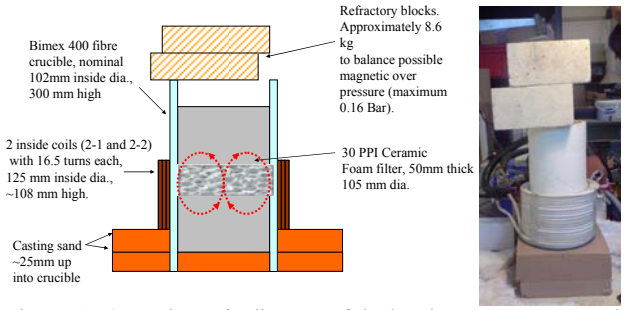

Figure 4. a) A schematic diagram of the batch test apparatus, and b) a photograph of the same.

In the meniscus experiments the coil was positioned in such a way that the bottom of the coil was in level with the top of the sand inside the fiber risers. In the batch filtration experiments, a CFF was cemented in at the junction of the two risers, as shown in Figure 4a). The coil was positioned in such a way that the mid-line of the coil (and the strongest point in the magnetic field) was in level with the bottom of the filter.

Alloy

A standard non-grain refined A356 alloy was used for the study of the meniscus behavior. The chemical composition of the alloy is given in Table II.

Table II. The chemical composition of the A356 alloy in wt. %.

Alloy type	**Si**	**Mg**	**Fe**	**Mn**	**Zn**	**Ti**	**Al**
A356	7.03	0.41	0.091	0.008	0.005	0.11	Bal

For the batch filtration tests a feed recipe was prepared containing: 60% A356 alloy, 20% anodized and lacquered plates, and 20% A356 composite material containing SiC particles with a size range 10-50 µm. For the meniscus tests, as well as the filtration tests, the alloy was melted in an induction oven at 750 ^{o}C.

Two filtration tests were conducted with 30 ppi CFF, i.e. one test with and one without a magnetic field, in the set-up shown in Figures 4a) and b). Maximum voltage was applied to the coil i.e. ~28 V, for ten minutes after pouring the molten metal. The power was then stopped and the sample solidified.

Results and Discussion

Meniscus tests

Four meniscus experiments and one batch filter test using magnetic field were conducted as summarized in Table III.

Table III. Summary of experimental results

Experiments	Coil	Voltage (V)	Current (A)	Total Power (W)	Load Power (W)	Magnetic Flux Density (T)	Theoretical Magnetic Pressure (Bar)	Liquid Metal Depth (mm)	Meniscus (mm)	Average Temperatue (oC)
1	1	14.21	364	4140	260	0.06	0.016	105	10	N/A
2	1 thicker insulation	27.96	684	16536	680	0.11	0.047	125	58	808
3	2 (1+2 in series)	28.15	730	11900	1270	0.20	0.16	108	70	774
4 meniscus	2 (1+2 in series)	14.40	373	3155	460	0.11	0.049	114	44	650
4 batch filter	2 (1+2 in series)	28.23	723	12200	1930	0.20	0.15	100 over and 100 under the filter	N/A	709

The aluminum was, as previously mentioned, heated to 750^{o}C and added to the unheated crucible where it cooled to ~710^{o}C. Coil 1, the traditional long coil, was used initially. In the first experiment the lowest available voltage (14 V) was used, and in the second experiment the highest (28 V). It was not known at the time if sufficient heating could be produced to hold the sample temperature at either voltage. The meniscuses produced in the first and second experiments are presented in Figure 5a) and b).

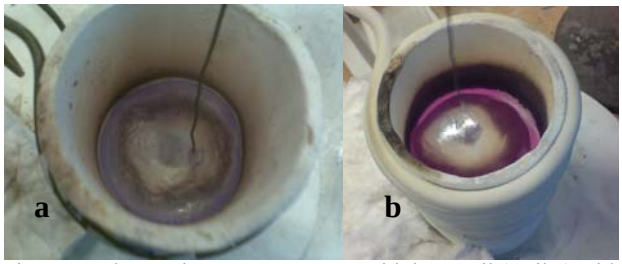

Figure 5. The meniscus measurement with long coil (Coil 1) with a magnetic flux density equal to a) ~0.06 T, and b) ~0.11 T.

It was established that the long coil (Coil 1) was just capable of compensating for heat losses at the lowest voltage, i.e. 14 V, with

260 W delivered for heating the sample. No temperature control was, however, possible. At the highest voltage, i.e. 28 V, 680 W was produced heating the sample to over 850°C within about 10 minutes. The power was periodically interrupted during the experiment to avoid excessive overheating.

Between experiments 1 and 2, it was found necessary to improve the electrical insulation of the coil, by the addition of a glass fiber sleeve. This caused the length of the coil to change slightly from 275 to 300 mm, and the inside diameter from 120 to 118 mm.

Based on the first experiments, it was realized that a more powerful magnetic field could be produced if the coil was shortened, and if a multi-layer coil was used (giving similar total conductor length and impedance). Fabricating a coil in segments gave more electrical flexibility, and better cooling could be achieved as the length of each segment was shorter and more cooling water could be supplied at the available line pressure.

The inner two layers of the multi-layer coil arrangement (Coil 2) were used in Experiments 3 and 4, first at the highest voltage and subsequently at the lowest. The meniscus formed at the highest magnetic field strength was reduced in diameter and increased in height as presented in Figures 6a) and b). Its motion was extremely dynamic, and it had a tendency to fall onto the side of the coil missing ½ of a turn.

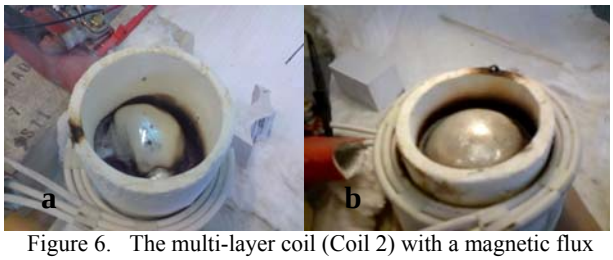

Figure 6. The multi-layer coil (Coil 2) with a magnetic flux density of a) ~0.20 T, and b) ~0.12 T.

The experimental data obtained from Experiment 3 and 4 are summarized in Table III. The meniscus heights as a function of the estimated magnetic flux density in the air gap between the coil and the work piece are plotted in Figure 7.

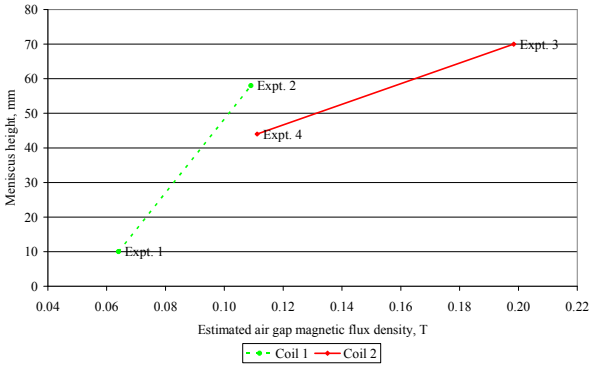

Figure 7. The obtained meniscus height (+/- 5mm) is plotted against the magnetic flux density estimated using Equation (2) for the long coil (Coil 1) and the multi-layer coil (Coil 2).

For the long coil (Coil 1) a greater meniscus height was created for a given magnetic flux density as the coil, and therefore the axial magnetic field, extended well beyond the aluminum pool. With the multi-layer coil (Coil 2), the aluminum was pushed up and partly out of the coil by the magnetic pressure. The observed meniscus height with the multi-layer coil, at the maximum transformer voltage, was sufficient to create back mixing through a filter depth of ~ 50 mm thickness.

Most of the Lorentz forces generated due to Equation (1) are dissipated due to viscous forces (flow) and this results in much less than the theoretically possible height increase in the liquid metal, as indicated in Table III (~10-30% of theoretical was observed).

Batch tests

In order to observe the largest possible difference between the gravity and the magnetic batch tests, the highest available voltage (~28 V) was applied to the coil to create the most powerful magnetic field possible. By adopting Equation (2), the magnetic flux density in the air gap between the coil and the work piece was estimated to be ~0.2 T.

The filter element was positioned in such a way that the bottom of the filter was located in the position of the highest magnetic flux density, as shown in Figure 1. It was believed that this would cause a maximum upwards flow through the filter element.

In the batch filtration tests it was found necessary to pre-heat the filter before starting the experiment to avoid an initial blockage under gravity conditions. Under the influence of the magnetic field preheating was, however, not required due to the resulting conditions caused by the field. The experimental data collected during the magnetic filtration experiment are also summarized in Table III.

During the batch test it was established, that with a sufficient metal height over the filter it was possible to avoid the formation of an excessive meniscus when under the influence of a stronger magnetic field. This experimental condition could be used to reduce the degree of oxidation and dross formation caused by the melt circulation. The degree of melt circulation was established to be so intense, that some of the sand from the bottom of the crucible was drawn from the sand base of the experimental set-up and dispersed into the liquid metal phase located beneath the filter, see Figure 4. Sand particulates were in fact lifted and pushed into the bottom of the filter element giving proof that intense back mixing was taking place during the experiment. The sand base at the bottom of the crucible remained, however, intact during the gravity filtration experiment. The cross section of the bottom part of the ingot with and without the influence of a magnetic field is presented in Figures 8a) and b).

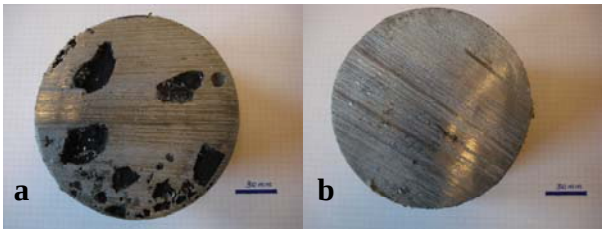

Figure 8. The cross section of the bottom part of the ingot obtained from the batch filtration tests a) with a magnetic field, and b) without a magnetic field.

The cross section of the filter media obtained from the experiments with and without a magnetic field is presented in Figures 9a) and b). In the sample influenced by the magnetic field it was established that the center part of the filter media at the top had been worn down as a result of the strong upward melt circulation through the filter. The filter media with the gravity pouring conditions showed, however no sign of degradation.

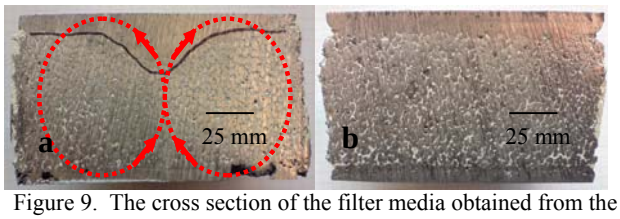

Figure 9. The cross section of the filter media obtained from the batch tests a) with a magnetic field, and b) without a magnetic field.

Representative Scanning Electron Microscope (SEM) micrographs of the filter cake with and without the influence of a magnetic field are presented in Figures 10 a) and b). It can be seen from the figure, that there are more SiC particles present in the filter cake in the sample poured under gravity conditions, while the SiC particle density is less in the sample poured and stirred with the magnetic field. It is assumed that the SiC particles, in this case, were more evenly dispersed due to the upward flow of the aluminum caused by the magnetic back mixing.

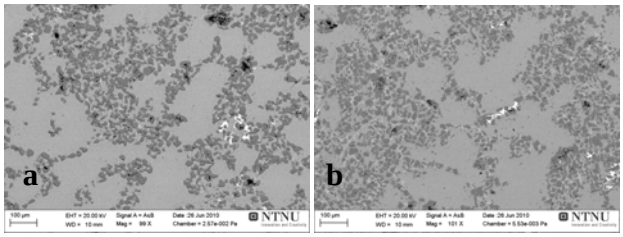

Figure 10. SEM micrographs of the filter cake a) with a magnetic field, and b) without a magnetic field (magnification X 100).

Conclusions

An experimental set-up has been designed and verified for the fluid re-circulation under different transformer voltages and coil designs. The largest meniscus height was observed using a multi-layer coil arrangement and a maximum transformer voltage of 28 V. Melt circulation under the influence of a magnetic field has proven to be effective in distribution of SiC particles.

Future Work

In industrial casting operations, a bulk flow field is produced in the filter by the gravity flow of metal, passing though the filter at a velocity of ~1 cm/s[13]. An example from the literature[14] is presented in Figure 11, indicating that a magnetic field should be capable of generating an internal flow velocity an order of magnitude greater than the normal industrial flow velocity range. Additional parametric studies will be conducted to explore the influence of the magnetic field on aluminum and inclusions flowing through a filter element.

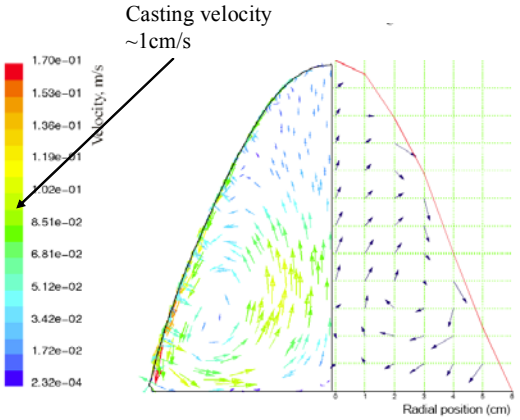

Figure 11. A simulation of the flow velocity and magnetic head produced in cold crucible experiments [14].

Acknowledgements

The authors wish to express their gratitude to Egil Torsetnes at NTNU, Trondheim, Norway, for helping with the design and construction of the experimental apparatus. Deepest gratitude is also due to Kurt Sandaunet at Sintef, Trondheim, Norway, for the use of the Sintef laboratory and his contribution in the execution of the experiments. Special thanks to Liss Pedersen at Alcoa, Lista, Norway, for the supply of filter materials. The author would also like to acknowledge the funding from the Norwegian Research Council through the RIRA project.

References

1. O. Majidi, S.G. Shabestari, and M.R. Aboutalebi, "Study of Fluxing Temperature in Molten Aluminum Refining Process", *Journal of Mat Pro Tech*, 182 (2007), 450–455.
2. B.W. Zhang, Z.M. Ren, and J.X. Wu, "Continuous Electromagnetic Separation of Inclusion from Aluminum Melt Using Alternating Current", *Trans Nonferrous Met SOC China,* 16(2006), 33-38.
3. K. Li, J. Wang, D. Shu, T.X. Li, B.D. Sun, and Y.H. Zhou, "Theoretical and Experimental Investigation of Aluminum Melt Cleaning Using Alternating Electromagnetic Field", *Materials Letters*, 56 (2002), 215– 220.
4. N. El-Kaddah, A.D. Patel, and T.T Natarajan, "The Electromagnetic Filtration of Molten Aluminum Using an Induced-Current Separator", *Journal of Materials*, 46 (1995).
5. Z.T. Zhang, Q.T. Guo, F.Y. Yu, J. Li, J. Zhang and T.J. Li, "Motion Behavior of Non-Metallic Particles Under High Frequency Magnetic Field", *Trans. Nonferrous Met SOC China*, 19 (2009), 674-680.
6. D. Shu , B. Sun, K. Li, and Y. Zhou, "Particle Trajectories in Aluminium Melt Flowing in a Square Channel Under an Alternating Magnetic Field Generated by a Solenoid", *Scripta Materialia*, 48 (2003), 1385–1390.
7. M.W. Kennedy, S. Akhtar, J.A. Bakken, and R.E. Aune, "Review of Classical Design Methods as Applied to

Aluminum Billet Heating with Induction Coils", submitted to EPD Congress 2011, TMS.
8. J. Vaughan and J. Williamson, "Design of Induction-Heating Coils for Cylindrical Nonmagnetic Loads," *American Institute of Electrical Engineers, Transactions of the*, 64, (1945), 587-592.
9. H. Nagaoka, "The Inductance Coefficients of Solenoids," *Journal of the College of Science,* 27, (1909), 18-33.
10. E. B. Rosa and F. Grover, "Formulas and Tables for the Calculation of Mutual and Self Induction," *Scientific Papers of the Bureau of Standards,* No. 169., (1916), 5-231.
11. H. Wheeler, "Simple Inductance Formulas for Radio Coils," *Proceedings of the IRE,* 16, (1928), 1398-1400.
12. D. Knight. (2010, August 25). *3.1. Solenoids: Part 1.* http://www.g3ynh.info/zdocs/magnetics/part_1.html
13. C. Dupuis, G. Béland, J.P., "Filtration Efficiency of Ceramic Foam Filters for Production of High Quality Molten Aluminum Alloys," (Paper presented at the 32nd Annual Canadian Conference of Metallurgists, 29th August – 2nd September), 1993.
14. E. Baake, A. Umbrashko, B. Nacke, A. Jakovics, and A. Bojarevics, "Experimental Investigations and LES Modeling of the Turbulent Melt Flow and Temperature Distribution in the Cold Crucible Induction Furnace", (Paper presented at the 4th International Conference on Electromagnetic Processing of Materials, Lyon, France, 14-17 October, 2003).